

# A Multi Compartmental model for Targeted Drug Delivery Based on Internet of Biological NanoThings

Islam R.Kamal

Department of pure mathematics and Computer Science, Faculty of Science, Menoufia University 32511 Egypt and Department of Computer Science, Modern Academy at Maadi, Egypt.

[Eslam.Ramadan@cs.modern-academy.edu.eg](mailto:Eslam.Ramadan@cs.modern-academy.edu.eg)

[islamkamal708090@gmail.com](mailto:islamkamal708090@gmail.com)

Saied M. Abd El-Atty

Department of Electronics and Electrical Communications Engineering, Faculty of Electronic Engineering, Menoufia University, Menouf 32952, Egypt.

[sabdelatty@el-eng.monfia.edu.eg](mailto:sabdelatty@el-eng.monfia.edu.eg)

[sabdelatty@gmail.com](mailto:sabdelatty@gmail.com)

S. F. El-Zoghdy

Department of Mathematics and Computer Science, Faculty of Science Menoufia University, Shebin El-Koom 32511, Egypt.

[Elzoghdy@science.menofia.edu.eg](mailto:Elzoghdy@science.menofia.edu.eg)

[elzoghdy@yahoo.com](mailto:elzoghdy@yahoo.com)

Randa F. Soliman

Machine Intelligence Department, Faculty of Artificial Intelligence, Menoufia University, Shebin El-Koom, 32511 Egypt.

[randa\\_soliman@ai.menofia.edu.eg](mailto:randa_soliman@ai.menofia.edu.eg)

[randafouad2010@yahoo.com](mailto:randafouad2010@yahoo.com)

**Abstract**—The authors propose a multi-compartmental model based on molecular communication (MC) technology for drug delivery to the malignant cell without affecting healthy cells in the patient's body. The medical personnel can transfer/control the required drug to the targeted cell with the help of a group of bio-nanomachines connected to the Internet of biological Nano Things (IoBNT) and a bio-cyber interface in both the forward and reverse directions. The proposed model consists of a set of multi-differential equations that are used to identify molecular communication among bio-nanomachines and quantify drug concentration to the targeted cell. Unlike conventional compartmental models, the proposed model can deliver the desired drug to the targeted cell by accounting for extracellular and intracellular tumor compartments, resulting in fewer therapeutic doses with improved efficacy. Simulations were also carried out to evaluate the performance of proposed multi-compartmental model with changing the physical parameters.

**Keywords**—Compartmental model, Drug delivery, Bio-nanomachine, Molecular communications, Internet of Bio-NanoThings.

## I. INTRODUCTION

Nanotechnology has introduced new concepts, methods, and devices that have the potential to improve existing technologies while also introducing entirely new scientific break throughs [1]. Based on the concept of changing materials at the molecular and atomic levels, nanotechnology can provide a small size device (nanomachine) that is bio-compatible for manipulating biomaterials at the system and organism levels. Sensing, catching, storing, releasing, and synthesizing biological molecules, obtaining, and expending energy, moving and actuating, and replicating/terminating are some of the functions of such bio-nanomachines have been described in [2]. For example, Doxorubicin (DOX) is a commonly used anticancer medication that can be used to treat a wide range of tumors. However, the DOX dose lifetime is limited due to the risk of cardio toxicity. This has prompted researchers to investigate the best dosing regimens for maximizing antitumor efficacy while avoiding cardio toxicity that is associated with plasma concentration [3]. As a

result, nanotechnology can provide nanoparticle (NP) drug carriers designed for delivery and release at the tumor site. Furthermore, nanotechnology recommends that molecular communication (MC) can be used to interconnect such bio-nano machines. On the other hand, the Internet of biological NanoThings (IoBNT) [4-11], which is based on bio-cyber interfaces, is a promising paradigm for connecting the MC environment with the external environment, such as the Internet.

Consequently, MC has potential applications in nanomedicine, where the topic of targeted drug delivery system (TDDS) is currently being extensively researched [12-14]. The goal of the TDDS, in particular, is to provide a specific drug where it is required (targeted site) while preventing the drug from negatively impacting on other sites of the body that are healthy [15]. A TDDS scenario based on MC is performed by a transmitter nanomachine which is used to emit the drug nanoparticle, which serves as information carriers. Furthermore, the blood plasma network acts as a communication channel, while targeted/tumor tissue acting as a receiver nanomachine [12,13]. The current work presents a multi compartmental framework for a targeted drug delivery system with help of IoBNT to control the therapeutic drug concentration by employing a bio-cyber interface model. The proposed framework helps to increase drug concentration in tumor tissues, resulting in fewer therapeutic doses, improved efficacy, less toxicity, and improved patient compliance and convenience, because it establishes two-way communication between medical personnel and bio-nanomachines that embedded in the human intra-body network. Furthermore, the bio-cyber interface will be designed for the IoBNT for interfacing with the external environment to control/adopt the concentration of drug particles within the targeted cell.

The remainder of the paper is organized as follows. Section II introduces the related work. Section III describes the proposed system model and the bio-cyber interface. Section IV presents the proposed multi compartmental framework in the forward and reverse direction for

broadcasting a molecular signal from the blood plasma network to the tumor network. Section V presents the simulation and numerical results of the proposed system. Finally, Section VI concludes the paper objectives and outcomes.

## II. RELATED WORK

Nanotechnology, information communication technology (ICT) and (IoBNT) are integrated to develop new drug delivery systems for drug targeting and hence providing a particulate (TDDS). The model presented in [16] introduces a descriptive scenario and system of the IoBNT that was used in an advanced healthcare delivery system. This model was utilized to address one of the IoBNT's main challenges by displaying the architecture and model of a bio-cyber interface for connecting a biochemical signaling-based nanonetwork to a conventional electromagnetic-based. In the other side, the Internet do not ensure that the drug reaches the target cell in the model presented in [16]. As a result, new values were added to ensure effective drug delivery to the targeted cell. This analysis focused on the system, which includes a bio-cyber interface and a blood vessel information propagation network that leads to the intra-body nanonetwork location. In [15], the authors have proposed MC-based TDDS for delivering the drug therapy to multiple sites in order to achieve TDDS effectiveness at diseased sites. The authors in [17] described a new TDDS paradigm, for the development of DOX drug delivery systems that enhance the therapeutic window (efficacy and safety) and address limitations of existing FDA-approved DOX formulations. In [3], a mathematical model for the cellular uptake and cytotoxicity of the anti-cancer drug DOX is presented. This model assumes sigmoidal, Hill-type dependence on drug-induced damage for cell survival. The results show that DOX cytotoxicity has distinct intracellular and extracellular mechanisms. Drug-induced damage is thus expressed as the sum of two terms, which represent the peak values of intracellular and extracellular drug concentrations over time.

Unlike the previous related work, wherein the authors had focused on delivering therapeutic drug molecules to infected cells at a specific site by using conventional compartmental model. This previous work did not employ the IoBNT model for actual controlling and delivering drug molecules to targeted sites and the elimination process. Thus, the proposed framework aims to carry out desirable therapeutic medications by employing multi-compartmental model. Furthermore, the proposed model regulates the concentration of drug molecules within the intended site and minimize negative effects on healthy cells in the same site by using multi compartmental model-based MC. The utilized MC uses a bio-cyber interface for the IoBNT paradigm to regulate the drug delivery system.

## III. PROPOSED SYSTEM MODEL

### A. System Model Description

Fig.1 depicts an illustrative example of the IoBNT modules that inspired by the previous work in [18], which will be developed in the proposed system model. We consider a healthcare delivery system scenario in which the (DOX) drug is delivered to the targeted cell (tumor cell) within the targeted tissue/site. In this scenario, the targeted nanonetwork consists of a group of therapeutic

nanomachines ( $nT_1$ ,  $nT_2$ ,  $nT_3$  and bio-nanosensor) have injected into the intra-body area network. A smart injection pump regulating the injection of DOX drug-loaded nanomachines or drug molecules is described in [16] while the transmission and propagation of DOX drugs can be accomplished by molecular communication system [13,14].

On the other hand, the bio-nanosensor senses the area inside the targeted nanonetwork to detect any chemical signal. Inspired by the biological cell structure, the therapeutic nanomachines have equipped by receptors for binding with the specific ligand (drug), thereby the reception process is performed according to the ligand-receptor binding mechanism. Additionally, therapeutic nanomachines are capable of transmitting and receiving data (i.e., transceiver nanodevices). Assume that  $nT_1$  is the transceiver bio-nanomachine (similar to PEGylated liposome) that encapsulates the desired drug, such as DOX, and has the ability to receive stimuli signal from the bio-cyber interface and thus emitting DOX drug. The  $nT_2$  and  $nT_3$  are bio-nanomachines that can also synthesize and release specific molecules to aid in the completion of the drug delivery system scenario. The proposed system model augments the IoBNT paradigm with a two-way bio-cyber communication interface to aid in careful instantaneous drug delivery to tumor tissue and investigates how nanoparticles (DOX drug) are exchanged among different bio-nanomachines. In the forward direction, the received binary command can drive the combinational logic circuit to produce a thermal or light signal which stimulates the  $nT_1$  (PEG liposome) to release the DOX drugs, while in the reverse direction, the bio-nanosensor detects bio-chemical signal produced by the bioluminescence reaction in the blood vessel and thus converted it to electrical signal. Hence, the bio-cyber transports the signal to medical personnel via the Internet. As a result, the main function of the bio-cyber interface is to connect the external network (such as the Internet) to the targeted nanonetwork (tissue).

As illustrated in Fig. 1, the signals  $x_1, x_2, x_3, x_4, x_5$  and  $x_6$  for the function IoBNT module, Internet, access point, wireless channel, bio-cyber interface, blood network, and targeted tissue respectively, can accomplish the communication sequence from forward to reverse direction and vice versa. The goal of proposed IoBNT-based MC system is to help medical personnel in the healthcare delivery system. The medical personnel are regarded as the remote storage, management, and maintenance of information pertaining to the regulation of DOX drug delivery system. To send a specific instruction, remote medical personnel use the wireless portal (access point) through which the bio-cyber interface connects to the remote medical personnel and the patient body via the Internet. Following that, the bio-cyber interface responds by sending the signal to the designated group of therapeutic bio-nanomachines within the targeted tissue via a vascular channel. The aim of therapeutic bio-nanomachines is to detect the malignant (tumor)site while causing no harm to the surrounding healthy tissues. As shown in Fig. 1, a bio-cyber interface receives the collected molecular information from the bio-nanosensor and thus converts it to an electrical signal in the reverse direction, whereas in the forward direction, the bio-cyber interface

converts the traditional electromagnetic (EM) wave to a bio-chemical signal. The signal stimulates the specific bio-nanomachine,  $nT_1$  (such as PEGylated liposomes), to release the stored nanoparticles (DOX drug) which can be diffused throughout the bloodstream and pass-through defective blood vessels that supply tumor intact.

Inspired by the conventional wireless communication system, the modules  $x_1(t)$ ,  $x_2(t)$ , and  $x_3(t)$  are the conventional IoT system and the module  $x_6(t)$  is group of bio-nanomachines and the bio-nanosensor in the targeted nanonetwork. We concentrate on the end-to-end physical layer structure in the proposed system model which is represented by  $x_3(t)$ ,  $x_4(t)$ , and  $x_5(t)$ . The effects of losses and errors in  $x_1(t)$  and  $x_2(t)$  caused by binary data transmitted by the medical personnel on the access point have been ignored. As a result, the communication channel was designed using  $x_1(t)$ ,  $x_2(t)$ , and  $x_3(t)$  as the output of the wireless communication channel  $z^n(t)$  as follows:

$$z^n(t) = y^{(n)}(t) * (x_1(t) * x_2(t) * x_3(t)), \quad n=\{f, r\} \quad (1)$$

where  $y^{(n)}$  is the input signal and  $*$  denotes the convolution operator. The superscript  $n$  indicates the type of communication direction, whereas the superscript  $r$  indicates the reverse communication direction (from the targeted tissue to the medical personnel) and  $f$  denotes the forward communication direction (from the medical personnel to the targeted tissue).

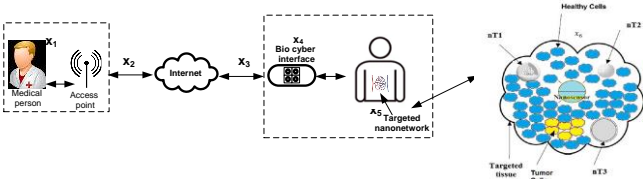


Fig. 1 System model descriptions: illustrative IoBNT-based MC system

### B. System Model Analysis

The proposed system model is mainly based on the architecture of bio-cyber interface [16]. As a result, we developed an interface consisting of a dual-transducing unit to decode a command message executed by an EM wave and then use that comm and to operate a transducer unit to generate a biochemical signal, as shown in Fig. 2. The developed interface depends on  $c^{(f)}(t)$  and  $c^{(r)}(t)$ , which represent the electrical and biological signals in the forward and the reverse direction, respectively.

In the forward direction, the received binary command can use the combinational logic circuit to produce a thermal or photo response which stimulates the  $nT_1$  (PEG Liposome) which releases the DOX drugs. In the context of molecular communications technology, the DOX drug as nanoparticles is stored in  $nT_1$  (liposome), which is thermal or photo sensitive. The output of the electro-bio unit,  $g^{(f)}(t)$  in the forward direction is given by:

$$g^{(f)} = \int_0^{R_{IN}} \xi \omega(t) dt, \quad \omega_0 = \xi \omega(t)|_{t=R_{IN}} \quad (2)$$

where  $R_{IN}$  is the time difference between the time of starting the injection process and the time of starting the

release of DOX drug and  $\xi$  infers the total number of liposomes in the system model. The concentration of DOX drug that is released at instant time  $t$  is represented by  $\omega(t)$ . We consider  $\omega_0$  is the value of  $g^{(f)}$  that is required at the targeted site.

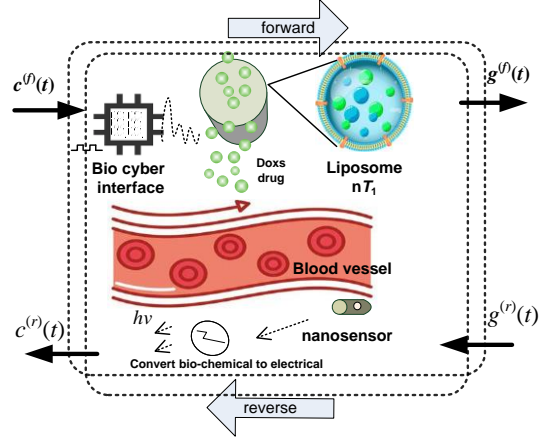


Fig. 2 The architecture of the developed dual bio-cyber interface.

The  $nT_1$  encapsulated DOX drugs are injected intravenously, passively propagate through the blood vessel network, and enter the targeted site in the proposed model. If the  $nT_1$  is stimulated by thermal or light stimulation at instant  $t$  (release time), the probability density function of DOX drug release by  $nT_1$  is expressed as [19]:

$$\omega(t) = d_t \omega_R (1 - e^{-\delta t}) \quad (3)$$

where  $\omega_R$  infers the released DOX drug concentration,  $\delta$  is the rate of release which is equal to the first-order rate constant, according to the type of the stimulation, we have two types of releasing rate for thermal or light time denoted by  $\delta_t$  and  $\delta_l$ , respectively, where  $\delta_t, \delta_l \in \delta$ . In (2),  $d_t = \frac{d}{dt}$  and  $\omega_R \approx \int_0^\infty \omega(t) dt$ . In the reverse direction, the bio-electro unit converts the biochemical signal detected in the blood network by the bio-nanosensor to electrical output. Due to a lack of drug molecules delivery, malfunctioning, or other causes, the bio-nano sensor detects variations in molecular data from the targeted cell and transmits it as a protein to the targeted site via the cardiovascular system.

The bio-cyber interface receives the released molecular information from the bio-nano sensor and converts it to an equivalent electric signal. Furthermore, the released molecular information from bio-nanosensor may be received by the receptors of the intravascular probe or diffused to excite the cellular pathway to activate them according to computed transcription factors, as shown in Fig.2. Based on the bio-luminescent reaction in [16], such reaction produces phosphate group (PP), adenosine monophosphate (AMP), and light  $h\nu$ . Thereafter, the bio-luminescence intensity,  $I(t)$  equation, including the Luciferase, (LU) and adenosine triphosphate (ATP), can be expressed according to the Michaelis–Menten mechanisms as follow [16]:

$$I(t) = \frac{\alpha_L L X}{X + \alpha_m} \quad (4)$$

where  $X$  and  $L$  are the concentration of ATP and LU, respectively.  $\alpha_m$  and  $\alpha_L$  are the Michaelis–Menten constant and catalytic reaction constant respectively. We can obtain the term  $L$  from the mRNA gene differential equations [20] and based on the Hill function in [21]. According to the interaction in the ligand-receptor mechanism presented in [22], we consider receptor mediated or direct diffusion of information molecules to be responsible for activating the transcription factor into the cellular structure that depends on the concentration of the diffusing information molecules, as opposed to [23] where the transcription factor was oscillatory input. As a result, we can represent the transcription factor concentration which describes the proposed bio-cyber interface as:

$$m(t) \approx \mu g^{(r)} \quad (5)$$

where  $g^{(r)}(t)$  is biological signals in the reverse direction and  $\mu$  denotes the signal conditioning at the cellular structure surface through which DOX drug diffuse.

#### IV. PROPOSED MULTI COMPARTMENTAL FRAMEWORK BASED MOLECULAR COMMUNICATIONS

The proposed model provides a more realistic perception by studying the effect of the drug molecules not only within the infected tissue(extracellular)but also within the infected cell(intracellular). As a result, it is possible to specifically target the infected cell without affecting the surrounding tissue. On the other hand, the previous studies were limited to demonstrating the efficacy of the vital destination, which operates on a two compartmental model. Furthermore, in the current study, we concentrated on a multi-compartmentalized model with a critical biocyber interface effect to increase the effectiveness, as shown in Fig. 3. depicts the flow diagram of MC in the blood vessel (or cardiovascular) network based on the proposed multi-compartment framework, where  $w_1(t)$  and  $v_1(t)$  represent DOX molecule concentrations in the forward and reverse directions, respectively. Furthermore, in the present study we focused on a multi-compartmentalized model under a vital biocyber interface effect to increase privacy and effectiveness, which is shown in Fig. 3. Further, we focused on delivering an accurate DOX drug to the tumor cell in the proposed model. The bio-cyber has been used to ensure the model's efficacy, and it can switch between a targeted nanonetwork within the human body and the Internet domain.

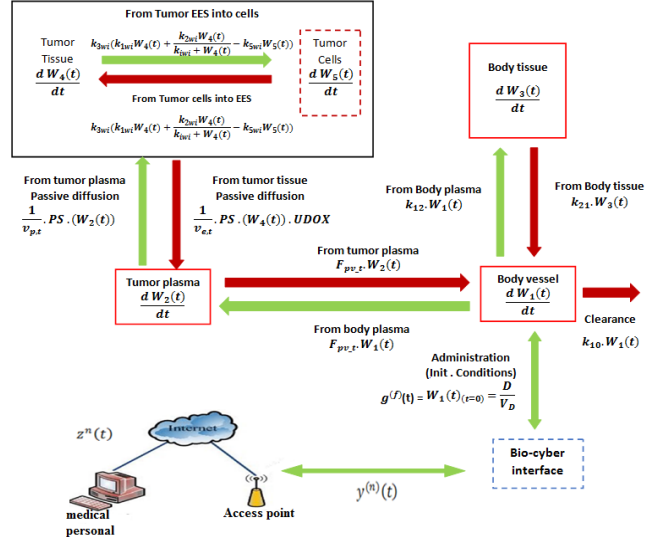


Fig. 3 Flow diagram of Proposed Multi-Compartmental Framework

##### A. The Forward Direction

The forward direction is considered from bio-cyber interface to the targeted nanonetwork. In order to develop DOX drug concentration, the following steps are performed:

- Step 1- A remote medical personnel send out command signal (in binary format) through the network.
- Step 2- This signal is picked up by bio-cyber interface that converts its EM wave to an appropriate bio-signal.
- Step 3- The drug is delivered to the blood vessel via the injection machine in the bio-cyber interface, where the DOX molecules are assembled and delivered to the tumor plasma, with both passive and active targeted being used to ensure that the treated molecules remain as long as possible to target the required cell without being attacked by the body's immune system.
- Step 4- The tumor plasma compartment transport drug to extravascular extracellular space (EES) of tumor tissues, the DOX drug transport by passive diffusion depending on the permeability surface area product, considering the different volumes of the tumor plasma compartment, EES and amount of drug which is transported between the plasma tumor compartment and the systemic plasma compartment by blood perfusion.
- Step 5- Finally, we assume two different concurrent intracellular uptake mechanisms are conducted of DOX: (1) passive diffusion across the cell membrane, and (2) an active transport mechanism, which is most likely, the drug received by the nano-transceivers in extravascular extracellular space (EES) of tumor tissues, and uptake by the tumor cells (targeted cell).

The molecular compartment model in the forward direction is derived by set of differential equations as follows:

$$d_t w_1(t) = -w_1(t)(k_{12} + k_{10}) + k_{21} w_3(t) \quad (6)$$

$$d_t w_3(t) = k_{12} w_1(t) - k_{21} w_3(t) \quad (7)$$

The equation described the rate of change of Dox in the body tissue compartment, where the first term is transfer from body vessel, second term is transfer to vessel.

where the subscripts 0, 1, and 2 indicate the position of the compartment. By considering the initial conditions:  $w_1(0) = g^{(r)}$  and  $w_2(0) = 0$ . The rate of change of drug concentration in the tumor plasma compartment is defined by:

$$d_t w_2(t) = -\frac{1}{v_{pt}} \times ps(w_2(t).UDOX) + \frac{1}{v_{pt}} \cdot ps(w_4(t).UDOX_e) - F_{pv_t} \cdot w_2(t) + F_{pv_t} \cdot w_1(t) \quad (8)$$

where the first term is the trans vascular transport by passive diffusion that is depending on the permeability surface area product  $ps$ , considering the different volumes of the tumor plasma compartment and EES. The second and third terms represent the amount of DOX drug which are transported between the plasma tumor compartment and the systemic plasma compartment by blood perfusion respectively.

On the other hand, the rate of change of concentration of free-DOX in the tumor EES is designated by:

$$d_t w_4(t) = \frac{1}{v_{et}} \cdot ps(w_2(t).UDOX) - \frac{1}{v_{et}} \cdot ps(w_4(t).UDOX_e) - k_{3w_1} \cdot \left( k_{1w_1} \cdot w_4(t).UDOX_e + \frac{k_{2w_1} \cdot w_4(t).UDOX_e}{(k_{1w_1} + w_4(t).UDOX_e)} - k_{5w_1} \cdot w_5(t) \right) \quad (9)$$

where,  $UDOX$  and  $UDOX_e$  denote the plasma binding for DOX drug and binding for DOX to proteins in EES respectively. In Equation 9, the first term describes the diffusion of drug within the EES, the second term describes the rate of transport of DOX from the tumor plasma space (transport= $PS \cdot UDOX(w_2(t) - w_4(t))$ ). The last term describes the rate of uptake of DOX into the tumor intracellular space, described by Equation 10:

$$d_t w_5(t) = k_{3w_1} \cdot \left( k_{1w_1} \cdot w_4(t).UDOX_e + \frac{k_{2w_1} \cdot w_4(t).UDOX_e}{(k_{1w_1} + w_4(t).UDOX_e)} - k_{5w_1} \cdot w_5(t) \right) \quad (10)$$

where, the first term explains the transport from tumor EES into the tumor cells. We assume two different concurrent intracellular uptake mechanisms of DOX: (1) passive diffusion across the cell membrane, and (2) an active transport mechanism, which is most likely endocytosis. Note that the intracellular uptake model likely varies for different cell types.

## B. The Reverse Direction

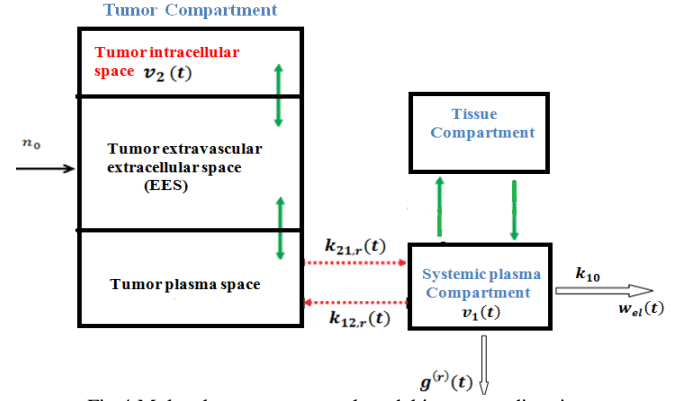


Fig.4 Molecular compartmental model in reverse direction

The concentration of DOX drug in each compartment is given by the ratio of the number DOX particles to the volume of the compartment. In the molecular compartmental model in reverse direction, in fig.4 the central compartment is the systemic plasma with the concentration of molecules termed by  $v_1(t)$ , while the concentration of particles in the tumor intracellular space is represented as  $v_2(t)$ . The function  $w_{el}(t)$  is the concentration of eliminated or biochemically modified molecules over time as a function of the elimination rate  $k_{10}$ . This concentration includes molecules that undergo phagocytosis, reaction process, and adhesion process, absorbed through non-targeted tissues, and eliminated by the liver as discussed in [16]. The parameters  $k_{12,r}$  and  $k_{21,r}$  are the first-order rate constants in or out of the targeted nanonetwork compartment, respectively. These rate constants are typically dependent on the concentration difference between the compartments, the size of the fenestra through the endothelia cell network, and the properties of the diffusing information molecules [24]. We consider the reverse of the conventional multi-compartment model; the rate equations can be described by:

$$g^{(r)}(t) = k_1 v_1(t) \quad (11)$$

$$d_t v_1(t) = k_{21,r} v_2(t) - (k_{12,r} + k_{10} + k_1) v_1(t) \quad (12)$$

$$d_t v_2(t) = k_{12,r} v_1(t) - k_{21,r} v_2(t) \quad (13)$$

where the term  $k_1$  is the ligand-receptor binding constant and  $k_{12,r}$  and  $k_{21,r}$  are the kinetic rate constants.

The  $v_1(0) = 0$  and  $v_2(0) = n_0$  are considered as initial conditions at  $t = 0$ . Additionally,  $n_0$  is the total concentration of the molecules emitted by the bio-nanosensor. Actually, we track the different transition states of the  $n_0$  via the IoBNT technology according to the expected value of  $I(t)$ , that translated by the bio-cyber interface to  $c^{(r)}(t)$ , where the value of  $c^{(r)}(t)$  is either 1 for  $I(t) \geq I_0$ , or 0 for  $I(t) < I_0$  according to (13).

$$c^{(r)}(t) = \begin{cases} 1 & I(t) \geq I_0 \\ 0 & I(t) < I_0 \end{cases} \quad (13)$$

## V. SIMULATION RESULTS AND DISCUSSIONS

In this section, the performance of the proposed multi compartmental model with IoBNT-based biocyber interface is evaluated. The performance evaluation considers delivering the DOX drug particles to the tumor (targeted)

cells while ensuring no side effects on healthy cells and the responsiveness of these cells prior to binding to the DOX drug. The effectiveness of the proposed framework in the forward and reverse directions is presented based on the efficacy of some parameters such as  $ps, k_{3w_i}, k_{12}, k_{21}$  and  $k_{10}$  with varying these parameters values on the reverse and forward directions. As well as the impacts of crucial design parameters such as  $\omega_0, \delta$ , and  $k_{12}, F_{pv,t}$  on the output  $w_2(t)$  are also evaluated. Python programming code was used to run the present simulation and evaluate the results. For each run, we employ the default settings shown in Table 1. Additionally, we used the results of earlier studies conducted in [16] to select the implementation parameters for each scenario.

Table 1. Default simulation values

Parameters	Description	Values
$\omega_0$	Drug concentration injected	0.7[16]
$k_{12}$	Kinetic constant	$9.4 \times 10^{-3}$
$k_{10}$	Elimination Rate	$2.1 \times 10^{-3}$
$k_{21}$	Constant from tissues to blood	$7.052 \times 10^{-5}$
$k_{1w_i}$	Parameter for intracellular uptake	2.257[3]
$k_{2w_i}$	Parameter for intracellular uptake	.0452[3]
$k_{3w_i}$	Parameter for intracellular uptake	$2.806 \times 10^{-3}$ [3]
$k_{5w_i}$	Parameter for intracellular uptake	10[3]
$k_{iw_i}$	Parameter for intracellular uptake	$5.29 \times 10^{-3}$ [3]
UDOX	Plasma binding for DOX	1.0
PS	Permeability surface area product for DOX	$4.9 \times 10^{-3}$ [25]
$F_{pv,t}$	Plasma flow in tumor plasma	0.30ml/min
$w_1$	Total does of encapsulated DOX injected	.7ml/mg [16]
$w_3$	concentration in Tumor plasma	calculated
$w_4$	concentration in Tumor Tissue	calculated
$w_5$	concentration in Tumor cell	Calculated
$V_{p,t}$	Volume fraction of tumor plasma spaces	0.0745 [26,27]
$V_{e,t}$	Volume fraction of tumor extracellular space	0.454
UDOX_e	Binding for DOX to proteins in EES	1.0

#### A. Performance Evaluation in Reverse Direction

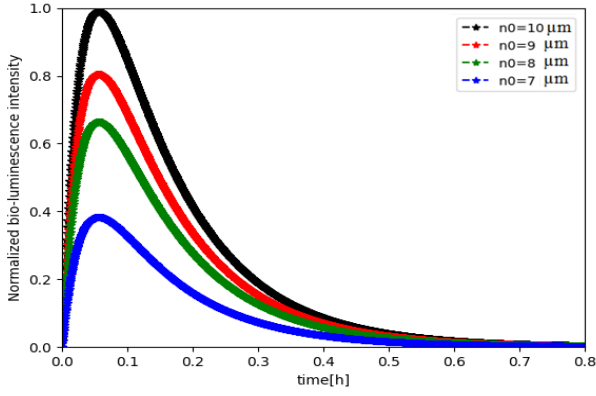
In this section, the performance of the normalized bio-luminescence intensity which provides the molecular information to the bio-cyber interface in the reverse direction of the proposed multi-compartmental framework is evaluated. In doing so, we selected the development of the evaluation parameters utilized in the previous experimental work [16]. The parameters values in the proposed multi-compartmental framework are:  $k_{21} = 7.052 \times 10^{-5} \text{ min}^{-1}$ ,  $k_{12} = 9.4 \times 10^{-3} \text{ min}^{-1}$  and  $k_{10} = 2.1 \times 10^{-3}$  [29];  $k_{12,r} = 0.103 \times 10^{-2} \text{ min}^{-1}$ ,  $k_{21,r} = 0.373 \text{ min}^{-1}$ ; and  $k_1 = 0.1 \times 10^{-2} \text{ min}^{-1}$ . We set  $\mu = 1$  by assuming that DOX drug molecules diffuse directly into the bio-electro transducer unit. The following factors for expressing LU are: the rate constant of translating mRNA into LU,  $k_r = 0.1 \times 10^2$  and  $k_p = 1.5 \times 10^2 \text{ h}^{-1}$  [29], the degradation rate of mRNA  $\gamma_r = 0.1005 \times 10^2 \text{ h}^{-1}$  and the degradation rate of LU

$\gamma_p = 0.0415 \times 10^2 \text{ h}^{-1}$  [30]. For the bio-luminescence reaction, values of the factors utilized are,  $\alpha_M = 15 \mu\text{M}$ ,  $\alpha_l = 0.044$  and  $a_{tp} = 0.04 \times 10^3 \mu\text{L}$  [31]. In the simulation, the noise variance applied is  $0.5 \times 10^{-1} \mu\text{M}$  [32].

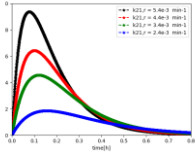
Additionally, in this work, the molecules follow the Brownian motion for moving in and out of the compartments and through the blood network. the concentration functions of the molecules,  $n_i(t)$  and  $w_i(t)$  include the Gaussian noise, specifically in this work, we use the normal distribution,  $N(0, \sigma_2)$ , zero-mean and variance  $\sigma_2$ . In analyzing the bio-luminescence intensity, we assume that the wavelength of the light emission is roughly constant, which is appropriate if the beam of light does not vary significantly. As a result, the photo resistor's sensitivity in the bio-cyber interface is mostly determined by the intensity of the emitted light. The value of  $\delta_l = 1.04 \times 10^{-4} \text{ min}^{-1}$  is used in our simulation procedure based on the experimental data in [34] for liposome exposure to ultraviolet light (UV). In the simulation, we used  $\delta_t = 0.0078 \text{ min}^{-1}$ [35] which was derived by utilizing the optimal curve for experimental data collected at  $42^\circ\text{C}$  using the non-linear least square method [36]. The effects of changing the values of  $n_0, k_{21,r}, k_1, \alpha_M, a_{tp}$  and  $k_{10}$  on the bio-luminescence density,  $I(t)$  described in arbitrary unit (a.u) for accomplishing the communication between the bio-cyber interface and medical personnel are shown in Fig. 5.

The results are obtained according to the derived equations in the reverse direction. We assume that  $I_0 = 0.007 \times 10^2 \text{ a.u}$  on the normalized scale. As shown in Fig.5(a), a low value of  $n_0$ , (for example less than  $8 \mu\text{M}$ ), is enough to send the electrical signal through bio-electro interface. As the result, to be accepted effectively at the bio-cyber interface, the bio-nanosensor must be able to release a large concentration of molecular information to increase the amount of concentration,  $n_0$  or it is required to use more than one bio-nanosensor.

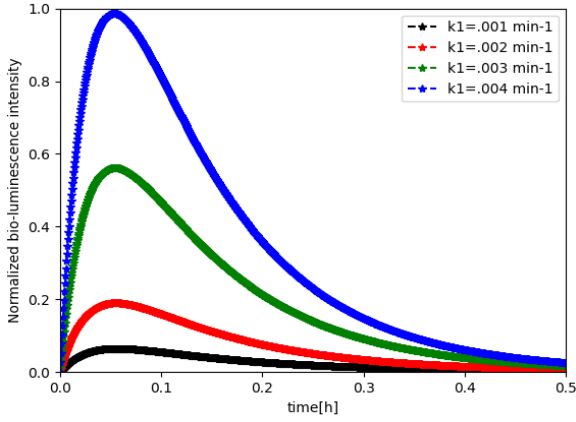
The variation in the reverse rate constant  $k_{21,r}$  has a substantial effect on bio-luminescence intensity, as shown in Fig. 5(b). As previously declared in the reverse direction, the scale of the fenestra in endothelial cell that regulates the transmission between the bloodstream and the targeted tissues effects on  $k_{21,r}$ . As well as the potentials of the diffusing molecular information, and the concentration difference between compartment  $v_2$  and  $v_1$ , have strong effect on  $k_{21,r}$  parameter. When  $k_{21,r}$  increases, the bio-cyber interface receives more molecular information, which results in increased bio-luminescence, as illustrated in Fig. 5(b). The bio-luminescence intensity increases significantly with sensible rate where the molecular information is observed by the bio-cyber interface, as illustrated in Fig. 5(c). This rate is determined by the receptor such that probes concentration or the distribution of porous membrane via which molecular information pass across the bio-cyber interface.



(a)



(b)



(c)

Fig. 5 Bio-luminescence density Variation with (a) concentration of  $n_0$ , (b) the diffusion rate constant  $k_{21,r}$ , and (c)  $k_1$ .

### B. Performance Evaluation in Forward Direction

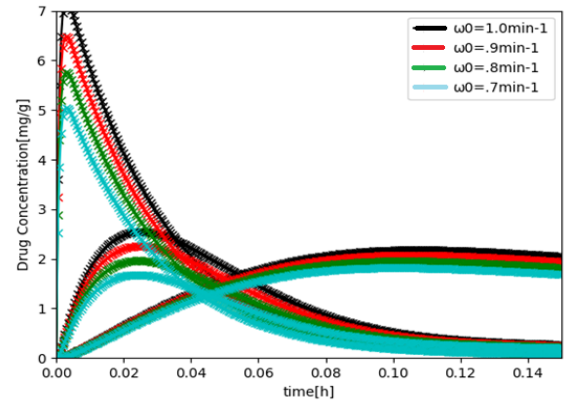
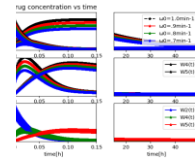
Fig. 6 depicts the effect of various parameters on the drug concentration bound for tumor cells. To achieve the desired results, we used (2) and (5) to (9). Also, Fig. 6 shows porosity values plotted against time. Table 1 also displays the simulation parameter values utilized in this investigation.

The fraction of injected  $\omega_0$ , which is  $g^{(f)}$  is controlled by the liposome release rate  $\delta$  and the period  $R_{IN}$  between the start of molecule release and injection time, as illustrated in Fig. 6(a). The effects of varying values of the injected molecules  $\omega_0$  from the bio-cyber interface encapsulated by liposome and spread within the blood vessel network  $w_1(t)$ .

are as illustrated in Fig. 6(a). Moreover, it can be shown in Fig. 6(a) that a higher concentration of molecule emitted increases the concentration of the drug molecules around the reception space of the targeted cell  $w_5(t)$  inside the targeted nano network (targeted tissue)  $w_4(t)$ . This means that the molecules emitted efficiently reach  $nT_2$  as drug molecules and increase their binding with the targeted cells before reaching  $nT_3$  which represents information molecules to eliminate the dose.

In Fig. 6(b), we can see how the variation in the elimination rate  $k_{10}$ , affects the results. Based on the results in Fig. 6, it is clear that  $k_{10}$  influences both the concentration of drug particles bound to diseased cells  $w_5(t)$  and, invariably, IoBNT. This means that a higher value of this parameter results in faster elimination, reducing both the peak plasma concentration and the duration of the effects. As a result, when designing IoBNT,  $k_{10}$  is an important parameter to be considered.

Fig. 6(c) shows how a higher constant forward rate  $k_{12}$  increases the concentration of drug particles around the reception space within the targeted tissues  $w_4(t)$ . Furthermore, Fig. 6(c) shows that this parameter is affected by the compartment differential, the scale of the fenestra that connects the nanonetwork to the blood network via the endothelial cell network, and the characteristics of the diffusing information particles.



(a)

effect of the forward cell uptake parameters  $k_{1w_i}$  inside the tumor cell. The parameters values of multi compartmental model that we used are listed in Table 1. In order to achieve an end-to-end secure channel for drug transport and delivery, our long-term goal is to secure IoBNT molecular information in the presence of cryptographic keys. Furthermore, we intend to apply biology blockchain technology to the IoBNT.

## VI. CONCLUSION

This paper presents a proposed compartmental model based on IoBNT technology that is based on a realistic potential scenario for improving targeted drug delivery system. We also present the proposed design model for the bio-cyber interface in the IoBNT. A multi-compartmental model for studying the implications and variations of drug concentration on disease cells (tumor cells) within the intra-body nanonetwork is also presented. The effect of changing physical parameters on the performance of the proposed system was investigated. The results show that reversing the system design parameters has a significant effect on drug concentration delivery.

## REFERENCES

- [1] I. Akyildiz, F. Brunetti, and C. Blázquez, "Nanonetworks: A new communication paradigm," *Computer Networks*, vol. 52, no. 12, pp. 2260-2279, 2008.
- [2] T. Nakano, T. Suda, Y. Okaie, M. Moore, and A. Vasilakos, "Molecular communication among biological nanomachines: A layered architecture and research issues," *IEEE Trans. NanoBio.*, vol. 13, no. 3, pp. 169-197, 2014.
- [3] A. W. El-Kareh, T. W. Secomb "Two-Mechanism Peak Concentration Model for Cellular Pharmacodynamics of Doxorubicin" *Neoplasia*, vol. 7, no. 7, pp. 705 – 713, July 2005.
- [4] S. M. Abd El-atty, "Health Monitoring Scheme-based FRET Nanocommunications in Internet of Biological Nanothings" *International Journal of Communication Systems*, vol. 33, no. 11, pp.1-17, July 2020.
- [5] A. El-Fatyany, H. Wang, M. Khan and S. M. Abd El-atty, "Biocyber Interface-based Privacy for Internet of Bio-NanoThings," *Wireless Personal Communications*, vol.114, no.2, pp. 1465-148, Sept. 2020.
- [6] A. El-Fatyany, H. Wang and S. M. Abd El-atty, "Efficient Framework Analysis for Targeted Drug Delivery Based on Internet of BioNanoThings," *Springer Arabian Journal for Science and Engineering*, vol.46, pp. 9965–9980, 2021.
- [7] M. Kuscuk and B. D. Unluturk, "Internet of Bio- Nano Things: A Review of Applications, Enabling Technologies and Key Challenges", *ITU Journal on Future and Evolving Technologies*, vol. 2, No. 3, 2021.
- [8] A. El-Fatyany, H. Wang and S. M. Abd El-atty, "On mixing reservoir targeted drug delivery Modeling-based Internet of Bio-NanoThings," *Springer Wireless Networks*, vol. 26, no. 5, pp. 3701-3713, July 2020.
- [9] S. M. Abd El-atty, N. A. Araf, A. Abouelazm, O. Alfarraj, K. A. Lizos and F. Shawki, "Performance Analysis of an Artificial Intelligence Nanosystem with Biological Internet of Nano Things", *CMES-Computer Modeling in Engineering and Sciences*, vol.133, no.1, pp. 111-131, 2022.
- [10] M. B. Dissanayake, and N. Ekanayake, "On the exact performance analysis of molecular communication via diffusion for Internet of Bio-Nano Things", *IEEE Transactions on NanoBioscience*, vol. 20, no. 3, pp. 291–295, 2021.
- [11] Q. L. Shen, J. Wu, J. H. Li, X. F. Zhang, K. Wang, "Communication modeling for targeted delivery under Bio-DoS attack in 6G molecular network". *IEEE International Conference on Communications*, pp. 1–5. Montreal, Canada. 2021.
- [12] Y. Chahibi, M. Pierobon, S.O. Song, and I.F. Akyildiz, "A molecular communication system model for particulate drug delivery systems," *IEEE Trans. Biomed Eng.*, vol. 60, no. 12, pp. 3468-3483, 2013.

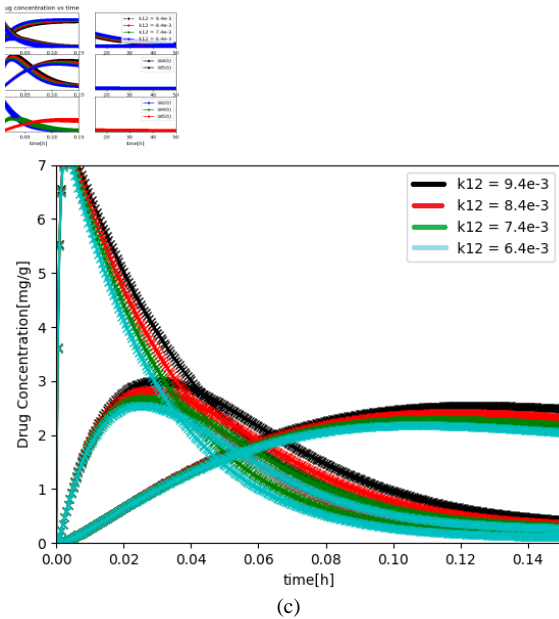
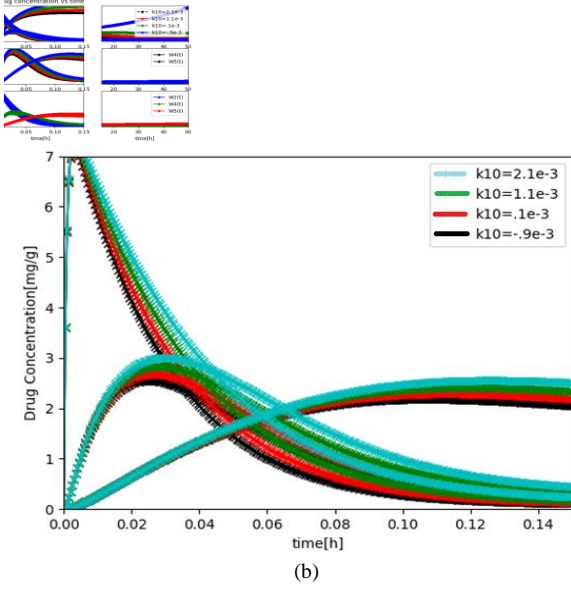


Fig. 6 Variation in  $w_2(t)$ ,  $w_4(t)$  and  $w_5(t)$  delivered to the intra-body nano-network with (a)  $\omega_0$ , (b)  $k_{10}$ , (c-d)  $k_{10}$  and  $\omega_0$ , (e)  $k_{12}$ , (f)  $k_{12}$  and  $\omega_0$ .

Furthermore, we investigate the performance of the proposed multi-compartmental model to demonstrate the

- [13] U. A. K. Chude-Okonkwo, "Diffusion-controlled enzyme-catalyzed molecular communication systems for targeted drug delivery," IEEE Global Communication Conference, Austin, Texas, Dec. 8-12, 2014.
- [14] Y. Chahibi, M. Pierobon, and I. Akyildiz, "Pharmacokinetic modeling and biodistribution estimation through the molecular communication paradigm," IEEE Trans. Biomed. Eng., vol. 62, no. 10, pp. 2410-2420, 2015.
- [15] U.A.K. Chude-Okonkwo, R. Malekian, and B.T. Maharaj, "Molecular Communication Model for Targeted Drug Delivery in Multiple Disease Sites with Diversely Expressed Enzymes," IEEE Trans. Nanobio., vol. 15, no. 3, pp. 1-1, April 2016.
- [16] U. A. K. Chude-Okonkwo, R. Malekian, and B. Maharaj, "Biologically inspired bio-cyber interface architecture and model for internet of bio-nanothings application," IEEE Transactions on Communications, vol. 64, no. 8, pp. 3444-3455, 2016.
- [17] N. A. Zhao, C. W. Martin, and A. J. Mixson, "Advances in delivery systems for doxorubicin" J. Nanomed Nanotechnol., vol. 9, no. 5, 519, 2018.
- [18] L. Ma, M. Kohli, and A. Smith, "Nanoparticles for combination drug therapy," ACS nano, vol. 7, no. 11, pp. 9518-9525, 2013.
- [19] M. Afadzi, C. Davies and Y.H. Hansen, "Ultrasound stimulated release of liposomal calcein," IEEE Conference on Ultrasonics Symposium (IUS), October 2010, pp. 11-14, San Diego, CA, USA.
- [20] M. A. Dollard, and P. Billard, "Whole-cell bacterial sensors for the monitoring of phosphate bioavailability," *Journal of Microbiological Methods*, vol. 55, no. 1, pp. 221-229, 2003.
- [21] G. Yagil, and E. Yagil, "On the relation between effector concentration and the rate of induced enzymesyn thesis," *Biophysical Journal*, vol. 11, no. 1, pp. 11-27, 1971.
- [22] S. M. AbdEl-atty, A. El-Taweel, and S. El-Rabaie, "Transmission of nano scale information based neural communication-aware ligand-receptor interactions," *Neural Computing and Applications*, vol. 30, no. 11, pp. 3509-3522, 2018
- [23] R. Vijayaraghavan, S. K. Islam, M. Zhang, S. Ripp, S. Caylor, N. D. Bull, S. Moser, S. C. Terry, B. J. Blalock, and G. S. Sayler, "A bioreporter bioluminescent integrated circuit for very low-level chemical sensing in both gas and liquid environments," *Sensors and Actuators B: Chemical*, vol. 123, no. 2, pp. 922-928, 2007.
- [24] B. G. Klein, *Cunningham's Textbook of Veterinary Physiology*, Missouri, USA: Elsevier Saunders, pp. 226, 2013.
- [25] T. L. Jackson, "Intracellular accumulation and mechanism of action of doxorubicin in a spatio-temporal tumor model", - *Journal of theoretical Biology*, vol. 220, no. 2, pp. 201-213, 2003.
- [26] F. Yuan, M. Leunig, D. A. Berk, R. K. Jain, "Microvascular permeability of albumin, vascular surface area, and vascular volume measured in human adenocarcinoma LS174T using dorsal chamber in SCID mice," *Microvascular research*, vol. 45, no. 3, pp. 269-289, 2003.
- [27] D. M. Brizel, B. Klitzman, J. M. Cook, and J. Edwards, "A comparison of tumor and normal tissue microvascular hematocrits and red cell fluxes in a rat window chamber model," *Bio. phys.*, vol. 25, no. 2, pp. 269-289, 1993.
- [28] S. Cascone, G. Lamberti, G. Titomanlio, and O. Piazza, "Pharmacokinetics of Remifentanil: a three-compartmental modeling approach," *Translational medicine@ UniSa*, vol. 7, no. 4, pp. 18-22, 2013.
- [29] C. M. Austin, W. Stoy, P. Su, M. C. Harber, J. P. Bardill, B. K. Hammer, and C. R. Forest, "Modeling and validation of autoinducer-mediated bacterial gene expression in microfluidic environments" *Biomicro fluidics*, vol. 8, no. 3, Art. ID. 034116, 2014.
- [30] T.S. Moon, C. Lou, A. Tamsir, B. C. Stanton, and C.A. Voigt, "Genetic programs constructed from layered logic gates in single cells," *Nature*, vol. 491, no. 7423, pp. 249-253, 2012.
- [31] K. Niwa, Y. Ichino, S. Kumata, Y. Nakajima, Y. Hiraishi, D. Kato, V. R. Viviani, and Y. Ohmiya, "Quantum yields and kinetics of the firefly bioluminescence reaction of beetle luciferases," *Photochemistry and Photobiology*, vol. 86, no. 5, pp. 1046-1049, 2010.
- [32] A.O. Bicen, and I.F. Akyildiz, "End-to-end propagation noise and memory analysis for molecular communication over microfluidic channels," *IEEE Trans. Commun.*, vol. 62, no. 7, pp. 2432-2443, 2014.
- [33] P. Bonate, "Advanced methods of pharmacokinetic and pharmacodynamic systems analysis," *IDrugsJ*, vol. 4, no. 9, pp. 1017-1020, 2001.
- [34] N.K. Sharma, and V. Kumar, "Release kinetics of novel photosensitive liposome for triggered delivery of entrapped drug," *PharmTech*, vol. 8, no. 1, pp. 106-113, 2015.
- [35] W. Zhan, and X. Y. Xu, "A mathematical model for thermosensitive liposomal delivery of Doxorubicin to solid tumour," *Journal of Drug Delivery*, vol. 2013, Article ID 172529, 2013.
- [36] T. Tagami, M.J. Ernsting, and S.D. Li, "Optimization of a novel and improved thermosensitive liposome formulated with DPPC and a Brij surfactant using a robust in vitro system," *Journal of Controlled Release*, vol. 154, no. 3, pp. 290-297, 2011